Predicting the pile static load test using backpropagation neural network and generalized regression neural network – a comparative study

Article *in* International Journal of Geotechnical Engineering · September 2018

DOI: 10.1080/19386362.2018.1519975

2 authors:

A. K. Alzo'ubi
Abu Dhabi University

Farid Ibrahim
Abu Dhabi University

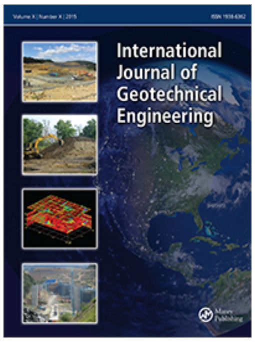

International Journal of Geotechnical Engineering

ISSN: 1938-6362 (Print) 1939-7879 (Online) Journal homepage: http://www.tandfonline.com/loi/yjge20

Predicting the pile static load test using backpropagation neural network and generalized regression neural network – a comparative study

A.K. Alzo'Ubi & Farid Ibrahim

To cite this article: A.K. Alzo'Ubi & Farid Ibrahim (2018): Predicting the pile static load test using backpropagation neural network and generalized regression neural network – a comparative study, International Journal of Geotechnical Engineering, DOI: 10.1080/19386362.2018.1519975

To link to this article: https://doi.org/10.1080/19386362.2018.1519975

Published online: 20 Sep 2018.

INTERNATIONAL JOURNAL OF GEOTECHNICAL ENGINEERING
https://doi.org/10.1080/19386362.2018.1519975

Taylor & Francis
Taylor & Francis Group

Predicting the pile static load test using backpropagation neural network and generalized regression neural network – a comparative study

A.K. Alzo'Ubi[a] and Farid Ibrahim[b]

[a]Civil Engineering Department, Abu Dhabi University, Al Ain, UAE; [b]Information Technology Department, Abu Dhabi University, Al Ain, UAE

ABSTRACT

In this paper, two neural network models; the Back Propagation Network, and the Generalized Regression Neural Network were built to predict the downward displacement of the entire static load test for Continuous Flight Auger piles. The models aim to increase our ability to predict the CFA pile's performance which depends on parameters such as the ground properties and the pile's characteristics. These parameters along with others were selected as input for a sample of more than six thousand field data points to train the two models. The models were then tested using three independent field tests and the results were matched against the actual measurements. The results showed that both models can predict the two loading-unloading cycles. To compare between the two models five statistical measures were used to show that the Back Propagation approach was more accurate than the Generalized Regression Neural Network while the latter was more precise.

ARTICLE HISTORY
Received 1 May 2018
Accepted 21 August 2018

KEYWORDS
Static load test; backpropagation neural network; generalized regression neural network; continuous flight auger piles

Introduction

In recent years, the construction industry in the United Arab Emirates (UAE) boomed and a large number of new projects has to be built as fast and as safe as possible. Sandy soils, which dominates the upper soil layers in the UAE (Fookes and Knill 1969), are very suitable for piling (Coduto, Kitch, and Yeung 2016). With this in mind, designers relied on the Continuous Flight Auger (CFA) piles to speed up the construction process. Performing quality control tests on these piles are mandatory and essential in the construction industry. After casting the piles for a project, 5% of them are randomly selected by the engineer to be tested (The Code Handbook: Abu Dhabi International Building Codes 2013). Usually, three tests are performed, namely: integrity test, dynamic load test, and static load test. In the latter, which is the focus of this study, the test load is usually applied in increments of up to 1.5 times the design load while monitoring the downward displacement. To avoid failure under static load tests, however, engineers tend to over-design these piles and multiple tests are normally needed to validate the design. Once the load reaches 1.5 times the design load, the test will stop and the displacement at that point will be compared with the standard. If the displacement of the pile exceeds the allowable displacement, the pile deems to be a failure and according to the UAE code of Building (The Code Handbook, 2013), all piles must be removed from the site. This means that all the piles considered in this country did not reach their ultimate capacity as the test was only performed to reach the 1.5 the design load.

In the field of geotechnical engineering, several Artificial Intelligence (AI) techniques, such as Artificial Neural Network (ANN), genetic programming, multivariate adaptive regression spline (MARS), support vector machine (SVM) were implemented. However, Shahin, Jaska, and Maier (2001) have pointed out that ANN is a powerful modelling tool in geotechnical engineering since such model can be trained on input–output data without the need to simplify the problem or incorporate assumptions. In addition, the results can always be improved by inputting new training data. Therefore, this research utilizes the ANN to predict the displacement at each point load to form the entire static load test curves. This will complement the current design approach, reduce the number of the required tests, and avoid the over-design issue. It is worth mentioning that while predicting the pile capacity and maximum displacement is a challenge; predicting the entire static load test curve is more challenging. Previous works in this field focused on predicting one point in the curve, which is the pile capacity and neglected the remaining points constituting the static load test. This might be attributed to three obstacles: setting up the network, number of parameters involved, and the amount of data available to train the network.

This approach would allow judging new proposed pile design ahead of the field tests, and the new tests would serve as new training data to improve future prediction accuracy and precision. This eventually will cut the cost of conducting multiple static load test for the same project. Coduto, Kitch, and Yeung (2016) stated that static load tests are much more expensive than analytical methods, and thus the latter is very attractive to be used by designers. However, the calculated load capacities are not as precise, so designs based solely on analytic methods must be more conservative and hence much more expensive than designs based on static load test results.

The data used in this paper were collected from hundreds of projects in three cities of the UAE; Abu Dhabi, Dubai, and Al Ain, as shown in Figure 1. To reduce the variation of the parameters in the models, three factors were considered: the

CONTACT A.K. Alzo'ubi abdelkareem@gmail.com Associate Professor, Civil Engineering Department Al Ain Campus, Abu Dhabi University, P.O. Box 1790, Abu Dhabi, United Arab Emirates

Figure 1. Location of the study area, United Arab Emirates.

consistency of the geology which reduces the geomaterial parameters variation; the dominant pile diameter; and the number of piles passing the tests. Only successful piles with 500 mm diameter were chosen since the majority of the 100 projects that were explored have this diameter and passed the static load test. The proposed model incorporates the soil profile, groundwater table, soil properties, the pile configuration and the load–displacement as the input parameters to the constructed networks.

Two ANN models, namely the Back Propagation Neural Network (BPNN) and the Generalized Regression Neural Network (GRNN), were trained over the collected data. The two models were then tested to predict a complete static load test of three independent projects. The results were compared with the actual field tests and then the two models accuracy and precision were measured. The comparative analysis showed excellent agreement between the actual field data and the predicted ones through different statistical parameters.

Backpropagation neural networks

The backpropagation neural network is one of the most commonly used training models in a variety of engineering applications. The model is based on processing a set of training records with known output by an algorithm to learn the neural network. It consists of three layers; input, hidden, and output layers. Each layer is composed of a set of units with weights assigned to connections to the next layers. To form the input layer, input attributes are simultaneously fed, weighted and passed forward to the next layer that may consist of one or more hidden layers to which initial weights and biases are also assigned. The number of hidden layers is experimentally specified and depends purely on the obtained result.

Each hidden layer produces an output that is propagated forward until it reaches the output layer where the network prediction value is obtained. The known output value of the current record is compared to the predicted value and the difference between the two values is considered an error. This error is propagated backward and weights and biases are adjusted for each unit in all layers. This process will iterate forward and backward and continue learning the values of the weights and biases until it approximates to a predicted output value that is within an acceptable error range. Once the model is built, it will apply the learned values of the weights and biases to process new input records and predict the unknown output (Han and Kamber 2012).

General regression neural networks

The general regression neural network applies regression to the input data using a probability density function. It is also a feedforward network consisting of four layers; input, pattern, summation, and output layers. All the attributes values are fed to the input layer as a vector. The pattern layer, consisting of units that store cluster centres, then receives these input. The cluster centres are determined using a particular clustering technique, such as the K-means. The objective of these centres is to group the sample inputs so that each group can be represented in one unit of the pattern layer measuring the distance of the input vector from the cluster centre (Specht 1991). The squares of all the differences between the values in a new vector and the cluster centres are summed and input to an activation function, which is an exponential function. The pattern layer produces an output, which is stored as two parts in the summation layer that consists of two units. The predicted value is produced in the output unit by computing the division of the stored values in the two summation units.

The main advantage of GRNN over BPNN is that it is simple and fast learning machine. This is because it does not need to back-propagate and iterate. The BPNN, on the other hand, requires extensive iterations in order to converge and produce the predicted output.

Previous work

ANNs were first used to predict the pile capacity in the 1990s, when Goh (1995) used a neural network model to estimate the friction capacity of driven piles in clay soils. The results were encouraging once compared to the actual data and some empirical equation. Later, Lee and Lee (1996) tried to predict the driven pile capacity by using an ANN model. The error between the predicted and the actual pile test was around 20%. Furthermore, Goh (1996) presented a new neural network model to predict pile capacity in sandy soils. The model's pile capacity was satisfactory when compared to other empirical formulas. In 1998, Abu Kiefa (1998) developed three ANN models to forecast driven piles capacity. One of these models used GRNN in predicting the ultimate capacity of driven piles in cohesionless soils. He compared the results with four empirical formulas and found that the model that was designated to forecast the total pile capacity was more accurate than others with 0.95 coefficients of determination. He also concluded that GRNN provided the best prediction for the pile capacity. Shahin and Jaska (2001) discussed different applications of ANN in Geotechnical Engineering and listed different applications including predicting the pile capacity.

Benali and Ammar (2011) also used ANN to anticipate the pile capacity; they used a database of 80 cases collected from the literature and corresponding to different sites distributed all over the world. They argued that their networks are feasible for these problems, we believe that for a different site far from each other this approach may not be accurate. More recently, Maizir and Kassim (2013) used ANNs for predicting the axial capacity of a driven pile; the data collected for this study consisted of 300 cases from several projects in Indonesia and Malaysia. They achieved good prediction whenever 'both stress wave data and properties of both driven pile and driving system are considered in the input data'. Alzo'ubi and Ibrahim (2017) proposed a framework for a model to predict the entire static loading test by using the backpropagation neural network.

Further models that utilized other AI techniques have all focussed on predicting the pile capacity. To predict the lateral load capacity of driven piles, Muduli, Das, and Das (2013) used extreme learning machine in addition to other neural networks models. The models were evaluated and ranked to identify the best model. Samui (2011) used SVM to predict the pile bearing capacity. He showed that the penetration depth ratio has the most significant effect on bearing capacity. In 2018, Mohanty, Suman, and Das (2018) used multi-objective genetic programming to predict the pile capacity of driven piles in cohesionless soil. They compared three AI techniques by using statistical parameters and presented three predictive model equations. Suman, Das, and Mohanty (2016) have applied many AI techniques to predict the friction capacity of driven piles in clay soils. Based on their statistical analysis, they reported that the MARS and functional network model have a better prediction capacity.

As shown in the above-mentioned studies, no attempt was made to predict the entire static load test, which is the focus of this study. Moreover, the previous studies focussed on driven piles which are rarely used in UAE, and no studies had been conducted on CFA piles, which are the most commonly used type in this country.

General geology and data gathering

The UAE lies on the floor of the Arabian Gulf, which mainly composed of extensive carbonate sediments. Fookes and Knill (1969) divided the mountain and piedmont plain of the Arabian Gulf into four sediment depositions. The coastline of UAE (Figure 1) is located in zone number four or the base plain. The upper layer deposits of this zone consist of sand dunes, loess, and evaporate together with marine sand and silts. Wind and evaporation, due to the high temperature, are the principal transporting agents in this region.

Although wind-blown material tends to predominate, as great quantities of silt and sand are moved during periods of high wind, water also plays an important role in this movement and later deposition of high quantities of Silty Sand material.

Flash floods, the last one was witnessed in 2015, are relatively rare, and any water stream actually reaching zone IV is usually short-lived after the rainstorm. However, the water table is very high and it can be as close as 0.5 m from the ground surface. This water table can dominate the desert processes by limiting the wind erosion to soils above the water table. As such, the groundwater table is incorporated as a parameter in the neural network models. Moreover, capillary pressure forces water movement from the water table to the ground surface as the water table is high and evaporation occurs at high rates.

In these conditions, a thick salt crust can build and it might affect the pile's performance. These deposits are common in the urban areas of UAE desert coastal regions and particularly extensive around this coastline. Beneath the first layers of sand and silt, other soil and rock materials exist. The Sand and Silt deposits cover interbedded sandstones, conglomerates, calcisiltite, limestone, and siltstones; clay deposits may also be encountered. Figure 2 shows a general subsurface profile commonly observed in the three cities.

To establish the subsurface conditions, 561 boreholes from Abu Dhabi, Al Ain, and Dubai were collected from the projects used in this research. Each static pile load test was then associated with the closest borehole in the same site to determine the variation of the soil properties along the pile shaft and later use these properties in the neural networks setting. The pile's length in all of the included projects ranges from 6 to 15 m, knowing that the depth of the Silty Sand layer ranges from 3 to 12 m and it plays a major role in establishing the pile performance due to friction. Undisturbed and disturbed split spoon samples were obtained from the boreholes by the geotechnical engineer to classify the soil and determine its properties. The sieve analysis and the Atterberg Limits tests were also conducted to classify the soil according to the Unified Soil Classification System to be used as a parameter in the Neural Network input data. In this research, the soil layers were categorized into 17 distinct layers and then coded as shown in Table 1.

Moreover, the friction between the geomaterials and the pile circumference area is an important factor that controls the pile performance in this kind of soil where cohesion is neglected. Consequently, the friction angle ($\emptyset'$) of the soil needs to be determined or estimated in order to be incorporated in the neural network. This value was obtained from laboratory test performed on undisturbed samples or calculated using the Standard Penetration Test (SPT) that was performed at every 1 m of depth in accordance with the

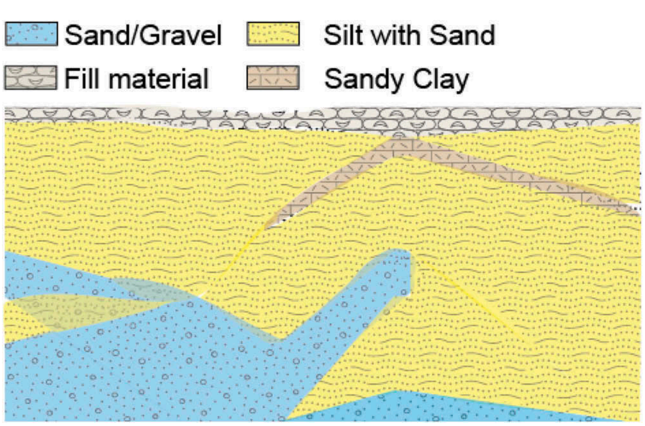

Figure 2. General subsurface profile found in Dubai and Abu Dhabi for the first 20 m below the ground.
(a) Reaction piles
(b) Testing in progress

Table 1. Soil classification and the soil profile codes used in the neural network model.

Soil profile	Soil description	Code
1	Silty SAND (SM): Dry to moist, light brown, fine non-plastic, trace fine gravel	10000000000000000
2	Poorly graded SAND with silt (SP-SM): Wet, light brown, fine, and non-plastic.	01000000000000000
3	MUDSTONE: Very weak to weak, moderately to highly fractured, moderately weathered.	00100000000000000
4	MUDSTONE: Weak moderately fractured, moderately weathered.	00010000000000000
5	Crystalline Gypsum: Moderately weak moderately fractured, moderately weathered.	00001000000000000
6	Loose to medium dense SAND with trace silt	00000100000000000
7	Very loose light brown clayey fine SAND.	00000010000000000
8	Dense, light brown fine silty SAND	00000001000000000
9	Weak, slightly conglomeratic CALCISILTITE, distinctly weathered (C), fracture close spaced	00000000100000000
10	Weak brown Sandstone mixed with Gypsum	00000000010000000
11	Medium dense to dense becoming very dense, gravely SAND	00000000001000000
12	Very dense, grey, very silty, fine to medium grained SAND	00000000000100000
13	Fine-grained, carbonate SAND with some amount of gravels	00000000000010000
14	Weak, slightly-moderately weathered, CALCARNITE.	00000000000001000
15	Very weak, light brown, poorly to well cemented calcareous SANDSTONE	00000000000000100
16	Medium dense, dry to moist, non-plastic, poorly graded SAND (SP)	00000000000000010
17	Very stiff, light grey, wet, non-plastic, sandy SILT (ML) with a trace of shells.	00000000000000001

ASTM D 1586 (ASTM, 2011) The SPT is considered reliable when performed in the granular material, such as those encountered in all of the projects in this research.

The SPT (N) values were used to calculate the friction angle (if not measured) such that, the raw N values were first corrected to 60% energy (N_{60}) to compensate for variation in the test procedures according to Skempton (1986):

$$N_{60} = \frac{E_m C_B C_s C_R N}{0.6} \tag{1}$$

where, E_m is the hammer efficiency, C_B is the diameter of the borehole, C_s is the sampler correction, C_R is a correction for the rod length.

Liao and Whitman (1985) suggested that for granular material, the N_{60} need to be further adjusted to take into consideration the effect of the overburden pressure. So the $(N_1)_{60}$ calculated from the previous step was modified by using:

$$(N_1)_{60} = N_{60}\sqrt{\frac{100\ kPa}{\sigma_z'}} \tag{2}$$

where σ_z' is the effective vertical stress at the SPT test location. The effective vertical stress was calculated based on the unit weight of the material at the corresponding depth.

To calculate the effective friction angle of soil, for soils that were not tested in the lab, the following formula that was suggested by Hatanaka and Uchida (1996) was used:

$$\varnothing' = \sqrt{20\ (N_1)_{60}} + 20 \tag{3}$$

Another important factor that controls the pile's performance, in addition to its skin friction, is its end bearing. Most of the piles in this research have reached the rock formation. Consequently, the Unconfined Compressive Test (UCT) of the rock was used as a parameter in the neural network. Samples of the rock layers were obtained using a double tube core barrel of 76 mm inside diameter and tested under uniaxial loading to determine the UCT value.

Static load test

According to the geotechnical engineer in all of the projects in this research, the recommended type of foundation was CFA piles. Figure3 shows the static load test setup in a tower near Zayed Port in Abu Dhabi. Pile load tests are considered the most satisfactory method to assess the performance of a pile under axial loading. In the UAE, it is mandatory to carry out the pile static load test during the foundation construction period according to the Building Code (The Code Handbook, 2013). Usually, the test is performed on randomly selected piles that are installed before the start of the general construction works. The common practice in the UAE is to test the piles for quality assurance and not for design; i.e. to check performance. As a result of this practice CFA piles, in most cases, are over-designed to avoid failure in the testing process.

In order to have a satisfactory design, Tomlinson and John (2014) established that for full skin friction mobilization, the pile needs to settle at least 1% of its diameter. While to mobilize the

a) Reaction piles

b) Testing in progress

Figure 3. Static load test by using reaction piles, Zaid Port, Abu Dhabi.

full end-bearing capacity, settlement of about 10% of its diameter is needed. Terzaghi (1943) and Meyerhof (1965) specified that the maximum vertical movement of a pile should not exceed 25 mm, no pile in this paper got even close to this value (the maximum measured total settlement was less than 4.0 mm). Also, according to the above discussion, a very small portion of the end-bearing resistance was mobilized if any. In addition, according to Das (2016), the maximum allowed residual settlement is 6 mm, this is to avoid pile failure for piles under 600 mm in diameter; no pile in this research has experienced this amount of residual settlement. So, to verify the pile performance and the load-displacement curves characteristics, the BSI (2015) was used as the testing procedure. The test load is applied in increments of up to 1.5 times the design load for working piles load. The load was applied by means of a hydraulic jack as shown in Figure 3(b), and four settlement gauges were used to monitor the downward displacement. In each increment stage, the load was increased and maintained for at least 20 min or until the rate of settlement decreased to less than 0.10 mm/h, whichever is greater.

The full static load test is obtained through two cycles. In the first loading cycle, increments of 25% of the design load – up to the working load – are applied at the tested pile and maintained until settlement seized. Settlement readings were taken every 5 min until the settlement stopped. In the first unloading cycle, the load was reduced in the inducement of 25% until zero and the settlement was recorded. The second reloading was then applied from zero to the test load (150% of the design load); first, increment from zero to the design load and kept until settlement seized. And then load was increased in 25% of the design load until the test load was reached. At the second unloading cycle, the load was decreased gradually in 25% steps until zero. In this research, all the static pile load tests were obtained through two cycles of loading–unloading.

Network topology, setting, and materials' properties

This paper aims to construct two models in which the downward displacement value can be predicted using BPNN and GRNN that are trained over data consisting of a combination of the soil profile and the pile configuration, as shown in Figure 4. Hence, if Si, SPi, DPi are assumed to be the soil profile value, soil properties value at depth DPi, P be the set of pile configuration whose parameters consists of {p1, p2}, then for an applied load Lj and a groundwater table G, it is possible to predict the displacement Dj such that *F*(Si, SPi, DPi, P, G, Lj) = Dj, where *F* is a mapping function for all load values of Lj in the pile test, and all Si, SPi values in a specified borehole. This mapping function is built using the two trained ANNs.

These input parameters are common between the two models and are shown in Table 2 along with their range of data. Moreover, Table 1 shows the soil profile, while Table 3 shows the status attribute values and their codes. To test the relevance of these parameters to the resulted output, a sensitivity analysis has been conducted to show how much an output changes when the inputs are changed during the experiment. After setting the inputs to the median values, the change in the output was measured as each input was increased from the lowest to the highest values to establish the sensitivity of the output to that change. Figure 5 shows the summary of the sensitivity of the input parameters in descending order. It is obvious from the figure that the output was affected by all input parameters with different degrees, except for the diameter which was fixed for all tests.

Table 2. Input attributes in the artificial neural network and their data types.

Attribute name	Data type	Data name	Values
Pile length (m)	Real number	PileL	6–15 m
Pile diameter (mm)	Real number	PileD	500 mm
Load (ton)	Real number	Load	0–165
Average displacement (mm)	Real number	AverageD	0–3.433
Status (loading–unloading)	Integer value	Status	2 cycles of each (see Table 3)
Groundwater GWD (m)	Real number	GWD	1.1–5.9 m
Depth (m)	Real number	Depth	0–17 m
Friction angle PHI (°)	Real number	PHI	27–43
UCT (kg/cm^2)	Real number	UCT	0–52.8
Soil profile (see Table 1)	Integer value	SoilPf	1–17

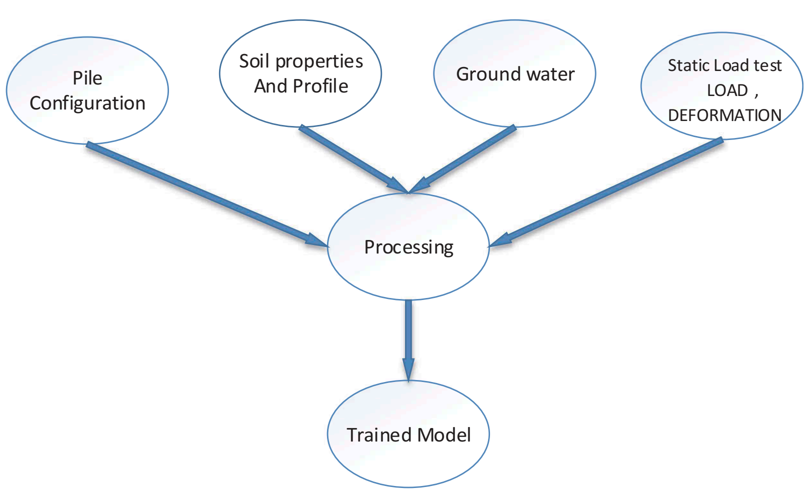

Figure 4. Training cycle in the artificial neural network used in this research.

Table 3. Codes for the loading–unloading cycles used in the training and testing cycles.

Status	Code value
First loading	1000
First unloading	0100
Second loading	0010
Second unloading	0001

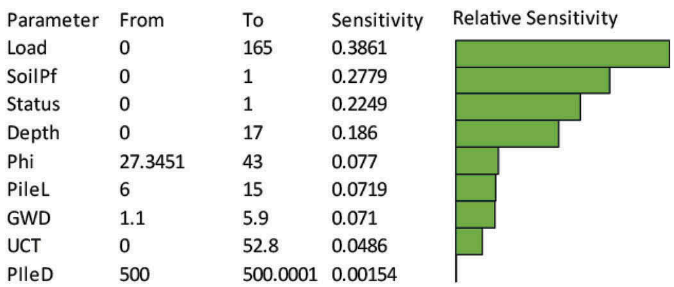

Figure 5. Sensitivity analysis of the input parameters.

The BPNN

A specialized software (Neural Planner Software 2016) was used to construct the BPNN, which consists of 28 input units; each corresponds to one parameter. The setting of the hidden layers was empirical where two hidden layers were chosen. There were 29 units in the first hidden layer and 15 units in the second. The initial weight setting was the default value of 0.6, the target training error was set to be 0.01 for all training records. Six-thousand four hundred thirty seven Pile data points were collected from the field, as described earlier, such that 5537 points were used for training and 900 random points were selected for validation.

Although the neural network software has different criteria to stop the training, two of which were used: all training errors are below the target error, or when the validation error starts to increase whichever comes first. The latter is called early stopping (Liu, Starzyk, and Zhu 2008; Prechelt 2012), which is necessary to avoid overtraining and consequently overfitting (Liu, Starzyk, and Zhu 2008; Haykin 1999). The produced model should generalize the mapping between input and output and should be capable of predicting the output for cases not included in the training set (Geman, Bienenstock, and Doursat 1992).

With this setting, the training stopped at the epoch of 5701 when the validation error was reported to be increasing. In this software, the average validation error value is considered as increasing when it is found increasing in six successive cycles. The values that were scored before training terminated, were as follows: 0.00088148, 0.00088566, 0.00089362, 0.00089493, 0.00090312, and 0.00090459. The average training error was 0.00053867, while the maximum training error was 0.03651359. Moreover, the predicted output points are distributed near the regression line for both the training and validation examples with R^2 of 0.9634 and 0.9675, respectively.

The GRNN

The GRNN model was constructed by implementing MATLAB Simulink 2017 software (MathWorks, 2016). The same set of input attributes shown in Table 3 were also selected. The same set of sample data, consisting of 6059 records, were migrated to MATLAB worksheet in order to generate a transposed matrix. The GRNN is then created using the command 'newgrnn (P,T) ' in the nntool, where P is the transposed input data and T is a vector storing the target displacement values. Two layers are created in this network. The first layer has as many units as there are inputs in P. The weight W in this layer is set to P'. The unit' s weighted input is computed as the distance between the input vector and its weight vector. The bias b is set to a column vector of 0.8326. The second layer has as many units as the target vector but with different weight setting W [28]. The training process in GRNN is very fast and has produced predicted values that are distributed near the regression line for the training examples with R^2 of 0.9574.

The test plan

After training the models, and to test the performance of the two approaches, three complete independent static-load tests from three different projects were chosen. The geotechnical data, the groundwater level, the pile configuration, the loading cycle, and the load were input, leaving the displacement field to be predicted. All of the three piles have 500 mm in diameter, while the length of the piles was 6, 7, and 8.5 m. For each of the chosen piles, the soil profile, the friction angle, the unconfined compressive strength, and groundwater level were also varied from test to test being chosen from three different locations, as shown in Table 4.

In the BPNN, a query file was created for each pile test and was individually processed by the model. Each row in the file is regarded as the input, and the model processed it to produce the predicted displacement. In this way, the displacement for each load was predicted independently. The load was increased in each successive row of the file in the same sequence as in the field test.

Similarly, the same chosen pile tests were selected for the GRNN model. To test the GRNN generated model (named 'net' here), MATLAB requires using the command 'sim (net, P) ' to produce the resulting output vector, where P is the input transposed matrix of the tested pile. The results of the two experiments are presented and discussed in the next section.

Results and discussion

The predicted displacement values produced at each load value in the three independent tests for the two models are presented and discussed with the aid of the following graphs:

- Actual vs. predicted displacement values to show the correlation and linear regression between them.
- Load vs. displacement values to show the difference between them at each increment/decrement of the two loading/unloading cycles.
- The residual plot and the average error

Displacement regression graphs

To show the displacement regression graphs, two criteria are used, namely precision and accuracy. Generally, the predicted

Table 4. Soil profiles for the three pile tests used in the query files to verify the ANN approach.

Test #	Depth (M)	Ø (°)	BH and its properties	UCT Kg/cm^2
Test 1	0.0	31.4	Silty Sand	0
	0.5	31.4	Silty Sand	0
	1.0	34.1	Silty Sand	0
	1.5	34.1	Silty Sand, G.W.T	0
	2.0	29.9	Silty Sand	0
	2.5	29.9	Silty Sand	0
	3.0	35	Calcarnite	13.5
	3.5	35	Calcarnite	13.5
	4.0	37	Calcarnite	17.2
	4.5	37	Calcarnite	17.2
	5.0	38	Calcarnite	19.1
		38	Mudstone	19.1
	5.5	42	Mudstone	43.1
	6.0			
Test 1	0.0	32.1	Silty Sand	0
	0.5	33	Silty Sand	0
	1.0	33	Silty Sand	0
	1.5	33	Silty Sand, G.W.T	0
	2.0	33	Silty Sand	0
	2.5	31	Silty Sand	0
	3.0	31	Silty Sand	0
	3.5	31	Silty Sand	0
	4.0	34	Calcarnite	12.1
	4.5	34	Calcarnite	12.1
	5.0	36	Calcarnite	15.3
		36	Calcarnite	15.3
	6.0	38	Calcarnite	19.3
	7.0			
Test 3	0.0	34.1	Silty Sand	0
	1.0	34.1	Silty Sand	0
	1.5	27.3	Silty Sand	0
	2.0	27.3	Silty Sand	0
	2.0	27.3	Silty Sand	0
	2.5	29.9	Silty Sand	0
	3.0	29.9	Silty Sand, G.W.T	0
	3.5	38.4	Silty Sand	0
	4.0	38.4	Silty Sand	0
	4.5	33.9	Silty Sand	0
	5.5	36.1	Silty Sand	0
		36.1	Silty Sand	0
	7.0	38.4	Silty Sand	0
	8.5	38.4	Silty Sand	0

and/or measured data once compared to the actual data can be: precise with low accuracy, low precision with low accuracy, and/or high precision with high accuracy as shown in Figure 6 (Wolf et al, 2014). The BPNN and the GRNN precision is measured by using the coefficient of determination, R^2, to show how far the predicted points from their regression line. Moreover, the accuracy was measured by using the best-fit equation of the data compared with the one-one line along with the coefficient of efficiency, E which is an unbiased statistical measure (Das and Sivakugan 2010):

$$E = \frac{E_1 - E_2}{E_1} \tag{4}$$

$$E_1 = \sum_{t=1}^{N} (S_a - \bar{S}_a)^2 \tag{5}$$

$$E_2 = \sum_{t=1}^{N} (S_{ann} - S_a)^2 \tag{6}$$

where N is the number of data points; S_a and S_{ann} are actual and ANN predicted settlement, respectively; and $\bar{S}_a$ is its average value. The calculation of E shows how far the predicted points are from the actual points.

The actual versus the predicted displacement graphs are plotted and presented in Figures 7–9 and Table 5. In terms of the model's accuracy, the BPNN model is more accurate than the GRNN; this accuracy is reflected in the best-fit equation of the three tests. The average slope of the one-one line is 0.9861 for the BPNN, and 1.1024 for the GRNN. Moreover, the BPNN has produced a better prediction of the actual displacement than the GRNN, not only for the average slope but also for each individual test. The unbiased coefficient of efficiency E, listed in Table 5, shows that both models are performing almost equally in test 1 and test 2 while BPNN outperforms GRNN in test 3. The reason for this difference will be further discussed in the next section. However, the graphs show that the GRNN is more precise than the BPNN;

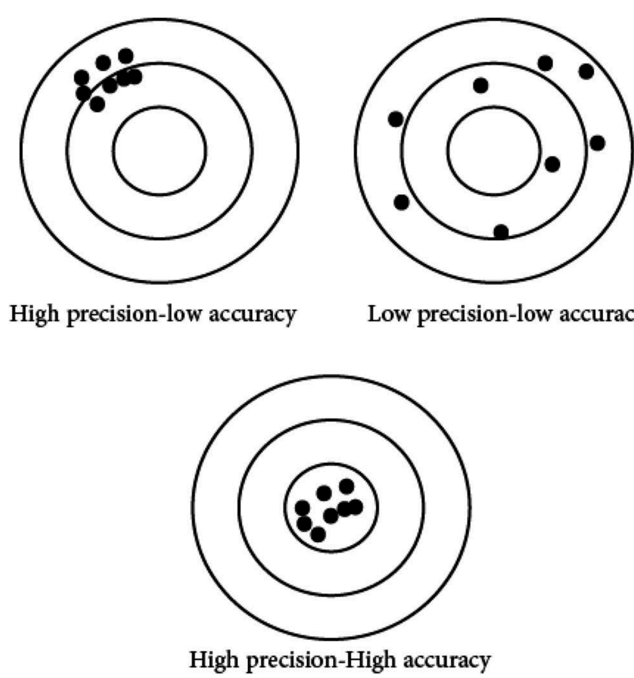

Figure 6. Accuracy vs. precision as used in this paper.

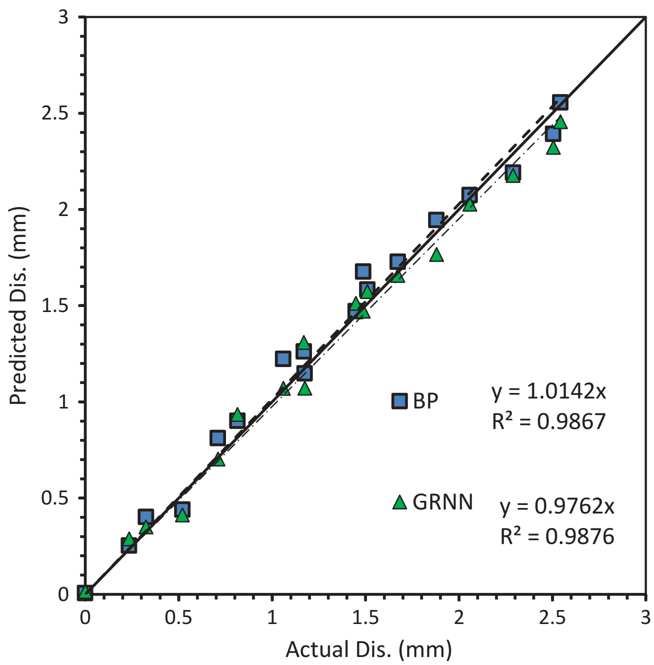

Figure 7. Actual vs. predicted displacement for both BPNN and GRNN networks, test 1.

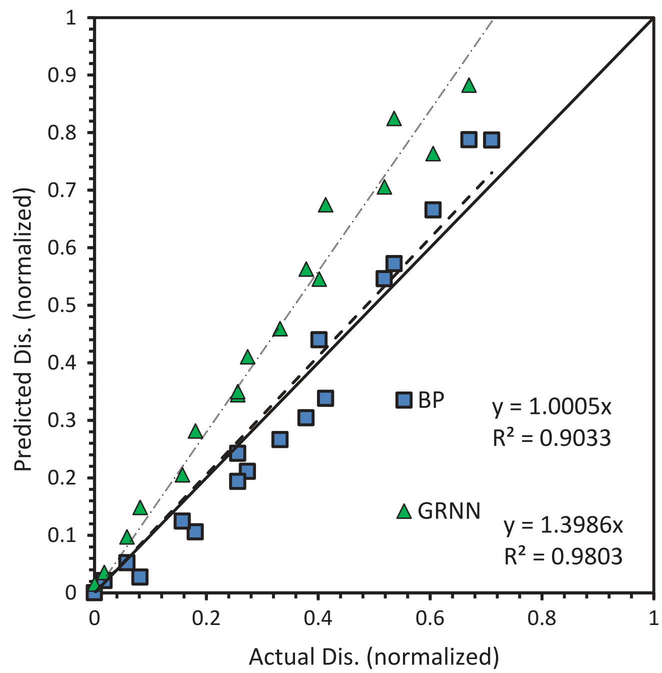

Figure 9. Actual vs. predicted displacement for both BPNN and GRNN networks, test 3.

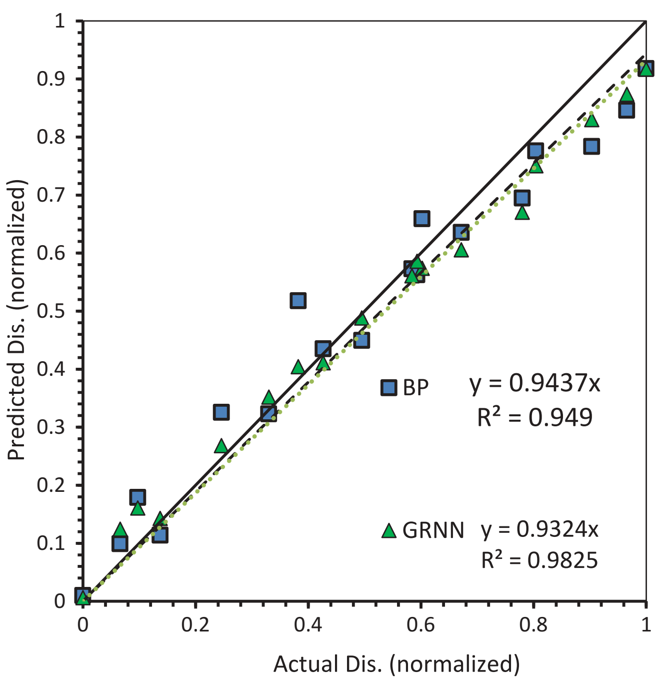

Figure 8. Actual vs. predicted displacement for both BPNN and GRNN networks, test 2.

Table 5. A comparison between the GRNN and BPNN, the best fit linear equation and the R^2.

	BPNN			GRNN		
	Equation	R^2	E	Equation	R^2	E
Test 1	Y = 1.0142 X	0.9867	0.9968	Y = 0.9762 X	0.9876	0.9968
Test 2	Y = 0.9437 X	0.949	0.9870	Y = 0.9324 X	0.9825	0.9922
Test 3	Y = 1.0005 X	0.9033	0.9788	Y = 1.3986 X	0.9805	0.8362

since R^2 of the former has an average value of 0.9835, while the average R^2 of the latter is 0.9463. Also, the R^2 of the GRNN in each of the three tests is higher than that of the BPNN. This could be because the GRNN relies on curve fitting technique and interpolation, rather than assigning different weights to the attributes as in the BPNN. The latter method operates in an iterative way until it achieves the acceptable error difference (Han and Kamber 2012).

Load vs. displacement

In the static load test, the pile is routinely subjected to two cycles of loading–unloading while monitoring the displacement. To further investigate the performance of the two networks with loading–unloading cycles, the two models' results were plotted along with the actual displacement as the load varies. This is shown in Figures 10–12. Although the two models produced reasonable results for the first two tests (Figures 10 and 11), the BPNN model, however, performed much better than the GRNN for the third test as shown in Figure 12. The GRNN has produced a larger error for the third test than the other two tests as illustrated in Figures 9 and 12. The reason for this marginal error was clear after investigating the training and the test data. It was found that there was not enough training data in the same displacement range for the third test (the maximum displacement measured in this test is 1.22 mm, while it is 2.505 and 2.773 mm in the other two tests). Such observation was also reported by Sarkar et al. (2015). However, this result was not observed in the BPNN model, as this method does not perform interpolation between similar points which is the case in GRNN. The GRNN is a one pass regression method that can produce little error if the testing data is within the range of the training data.

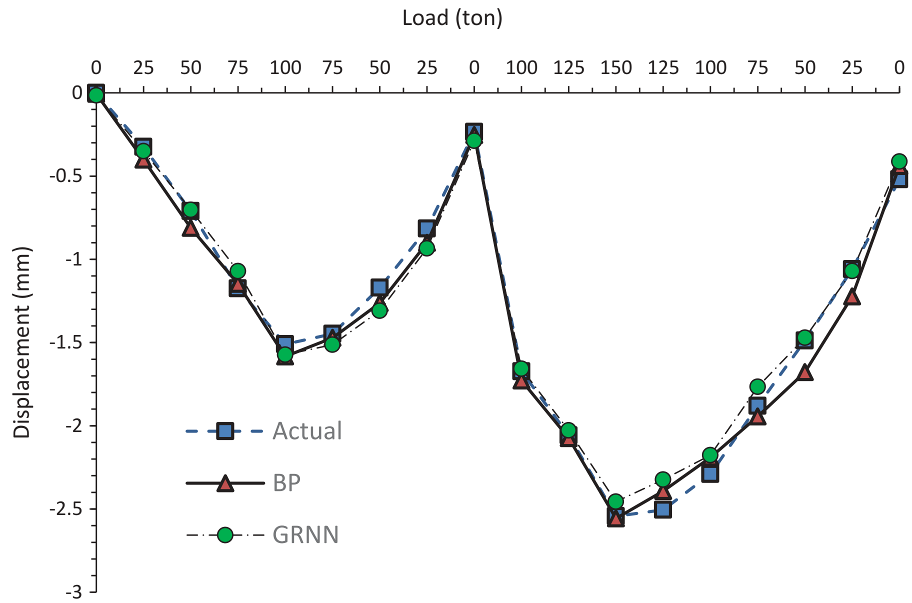

Figure 10. Two cycles of loading–unloading static load test curve for both BP and GRNN methods, test 1.

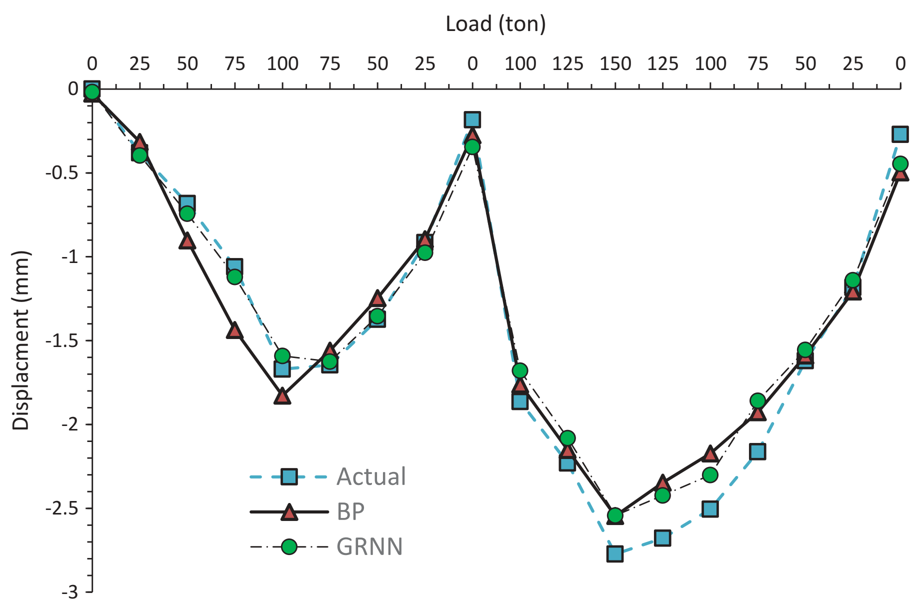

Figure 11. Two cycles of loading–unloading static load test curve for both BP and GRNN methods, test 2.

Measurement of models error

The residual plots for each of the three tests in both models are presented in Table 6. For the GRNN, the table shows that this model tends to overestimate the predicted displacement on the average. This observation is most obvious in test 3 in Table 6 where all the points were overestimated. Kurup and Griffin (2006) also reported that GRNN overestimates the predicted values when the test data falls close to the training data. In this paper, the testing displacement and the output displacement are very close to each other (the range is within 3 mm in all tests. For the BPNN, Table 6 shows that the residual values are distributed above and below the horizontal axis, which indicate that the displacement values are randomly dispersed.

The average percentage error in the predicted displacement at each load for the three tests was also calculated and plotted as shown in Figure 13 for both models. It is obvious, from Figure 13, that the BPNN model produced lesser error than the GRNN at each load. It is also worthwhile to mention that GRNN tends to overestimate the displacement along the entire range of the loading path. The average errors of GRNN and BPNN across the data were 17% and 1%, respectively. The maximum error occurred in the third test as was shown in Figure 13 and for the reason indicated in the previous section.

Conclusion

In this paper two neural models were developed, the BPNN and the GRNN, to predict the static load test by using the material properties, groundwater table, and the pile configuration as input parameters. The two networks have

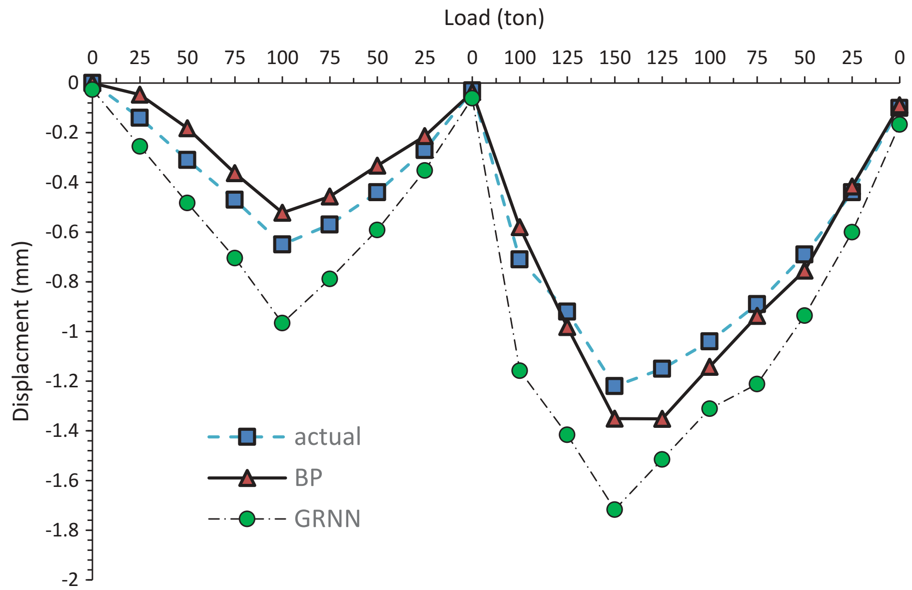

Figure 12. Two cycles of loading–unloading static load test curve for both BP and GRNN methods, test 3.

reasonably predicted the static load test, however, the BPNN was more accurate than the GRNN which was observed to be more precise. This performance might be attributed to the amount and range of data available to train the model. The amount of data available to train the network plays an important role if GRNN is to be used since it cannot estimate a point outside the range of the trained data. Furthermore, with the same quality and quantity of data, the BPNN produced better results than the GRNN.

This research showed the possibility of predicting the entire static load test rather than only the pile capacity as it was the focus of other studies. As shown in the

Table 6. Residual plots for the three tests of both ANN models.

Test	BP	GRNN
Test one	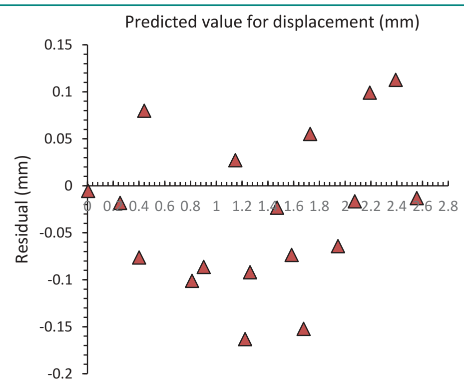	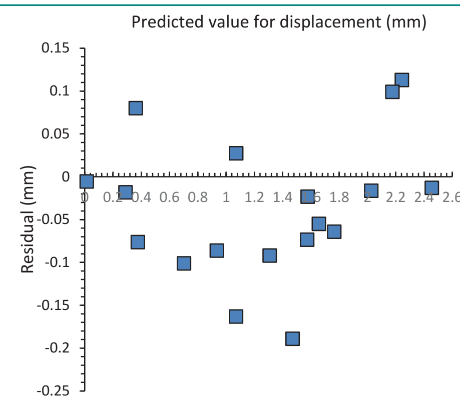
Test two	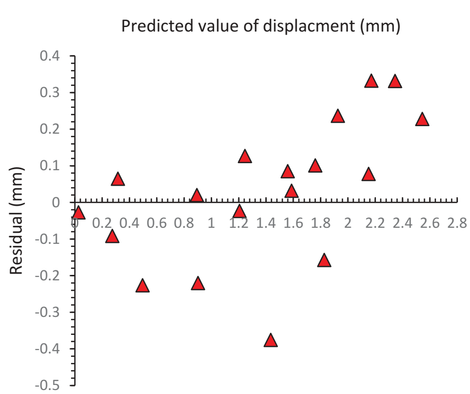	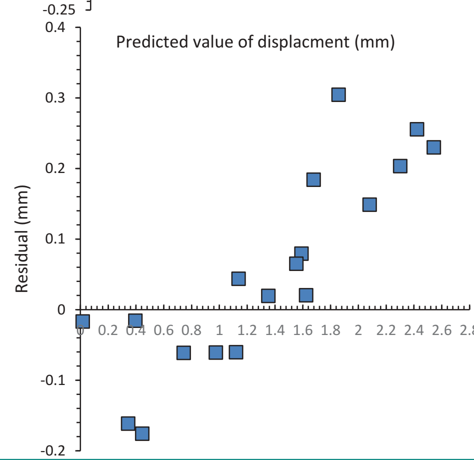

(*Continued*)

Table 6. (Continued).

Test	BP	GRNN
Test three	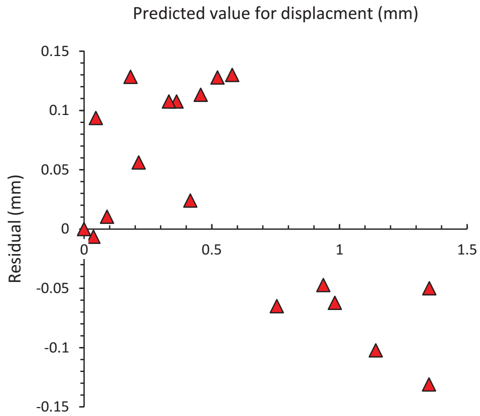	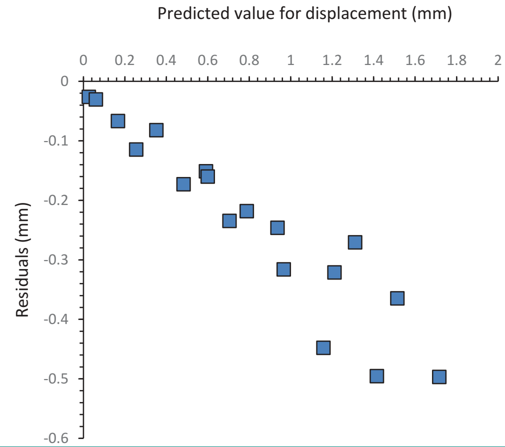

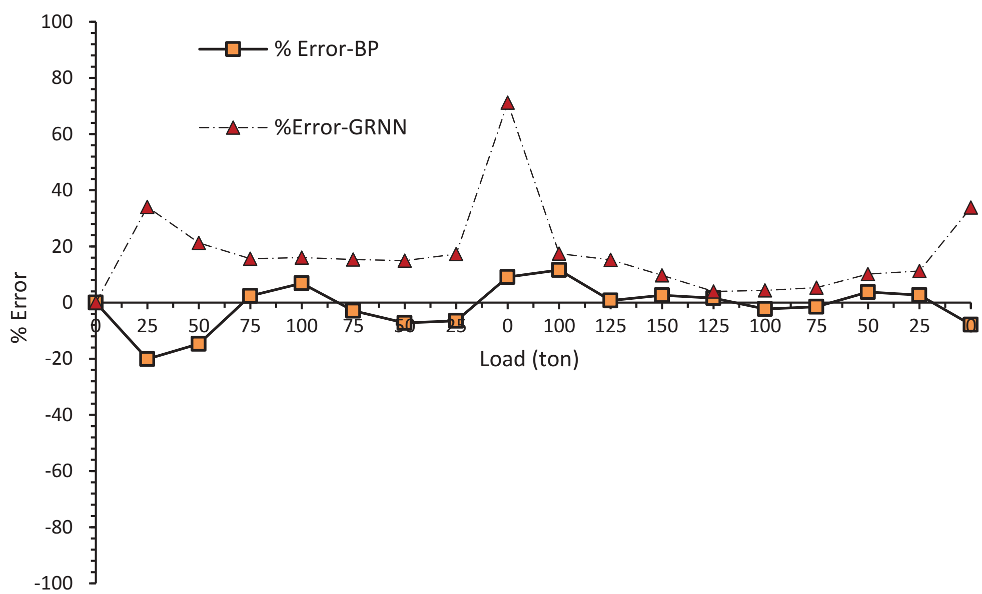

Figure 13. The average error calculated from three tests for both BPN and GRNN.

statistical analysis, the results were encouraging so that with a sufficient amount of data, neural network models can be built to complement the current pile test methods. Consequently, the cost of performing multiple pile tests can be reduced.

Acknowledgments

The authors would like to extend their gratitude to the office of scholarship and sponsorship programs at Abu Dhabi University for their financial support of this project (Grant No. 19300093).

Disclosure statement

No potential conflict of interest was reported by the authors.

Funding

This work was supported by the Abu Dhabi University [19300093].

Notes on contributors

Dr. Abdelkareem Alzo'ubi is an Associate Professor at Abu Dhabi University with a Ph.D. from the University of Alberta, Edmonton, Canada and he is a licensed Professional Engineer in Canada. His research interests are Numerical modeling of geo-material by using Hybrid techniques, underground tunneling, and slope stability. Laboratory research and testing are at the core of his interests in addition to deep foundations and artificial intelligence in Geotechnical Engineering. During the last seventeen years, he has conducted extensive research on new numerical approaches to model the behavior of soil and rock masses and behavior of deep foundation. Dr. Alzo'ubi is an expert in infrastructure modeling, he was recognized for his work in those areas through a number of awards and scholarships. Dr. Alzo'ubi holds several

grants from Abu Dhabi University to fund graduate and undergraduate research and He is currently the president of MEROCKS.

Dr. Farid Ibrahim is an Assistant Professor of Computer and information sciences at the college of Engineering - Abu Dhabi University. The main theme in his Ph.D. research was computational linguistic techniques in information retrieval applied to the Arabic language. He holds the position of the college coordinator in Al-Ain campus of the university since 2009. Besides his administrative duties in this university and other previous universities, he has published a number of papers in the field of computation of Arabic linguistics; testifying and improving coding schema for Arabic, developing sorting and searching algorithms using such a schema. Lately, he started a research interest in the application of neural networks as a prediction model for the pile static load test. He has also conducted a similar model to predict the diagnosis of chronic diseases like diabetes. Moreover, he has also been engaged in a variety of committees for curriculum development in the fields of computer science and information systems for both the undergraduate and postgraduate levels

ORCID

A.K. Alzo'Ubi http://orcid.org/0000-0003-3449-7089
Farid Ibrahim http://orcid.org/0000-0002-4245-4604

References

Abu Kiefa, M. A. 1998. "General Regression Neural Networks for Driven Piles in Cohesionless Soils." *Journal of Geotechnical and Geoenvironmental Engineering - ASCE* 124 (12): 1177–1185. doi:10.1061/(ASCE)1090-0241(1998)124:12(1177).

Alzo'ubi, A. K., and F. Ibrahim. 2017. "Towards Building a Neural Network Model for Predicting Pile Static Load Test Curves." 2nd International Congress on Materials & Structural Stability CMSS-2017, Rabat, Morroco, 22-25 Nov. 2017, MATEC Web of Conferences 149, 02031 (2018), doi:10.1051/matecconf/201814902031

ASTM D1586-11. 2011. *Standard Test Method for Standard Penetration Test (SPT) and Split-Barrel Sampling of Soils*. West Conshohocken, PA: ASTM International. www.astm.org.

Benali, A., and A. Nechnech. 2011. "Prediction of the Pile Capacity in Purely Coherent Soils Using the Approach of the Artificial Neural Networks." In International Seminar, Innovation & Valorization in Civil Engineering & Construction Materials, N °: 5O-239, University of sciences and technology, Algiers, Algeria.

BSI (British Standards Institution). 2015. *BS 8004, Code of Practice for Foundations*. London, UK: BSI.

The Code Handbook: Abu Dhabi International Building Codes. 2013. *Department of Municipal Affairs*. Abu Dhabi: UAE.

Coduto, D. P., W. A. Kitch, and M. R. Yeung. 2016. *Foundation Design, Principles and Practices*. 3rd ed. Upper Saddle River, NJ: Prentice Hall.

Das, B. 2016. *Principles of Foundation Engineering*. 8th ed. Boston, MA: Cengage Learning.

Das, S. K., and N. Sivakugan. 2010. "Discussion Of: Intelligent Computing for Modelling Axial Capacity of Pile Foundations." *Canadian Geotechnical Journal* 47: 928–930. doi:10.1139/T10-048.

Fookes, P. G., and J. L. Knill. 1969. "The Application of Engineering Geology in the Regional Development of Northern and Central Iran." *Engineering Geology* 3: 81–120. doi:10.1016/0013-7952(69)90001-5.

Geman, S., E. Bienenstock, and R. Doursat. 1992. "Neural Networks and the Bias/Variance Dilemma." *Neural Computing* 4: 1–58. doi:10.1162/neco.1992.4.1.1.

Goh, A. T. C. 1995. "Empirical Design in Geotechnics Using Neural Networks." *Geotechnique* 45: 709–714. doi:10.1680/geot.1995.45.4.709.

Goh, A. T. C. 1996. "Pile Driving Records Reanalyzed Using Neural Networks." *Journal of Geotechnical and Geoenvironmental Engineering - ASCE* 122 (6): 492–495. doi:10.1061/(ASCE)0733-9410(1996)122:6(492).

Han, J., and M. Kamber. 2012. *Data Mining, Concepts and Techniques*. 3rd ed. MA, USA: Morgan Kaufman Publishers.

Hatanaka, M., and A. Uchida. 1996. "Empirical Correlation between Penetration and Resistance and Internal Friction Angle of Sandy Soils." *Soils and Foundations* 36 (4): 1–10. doi:10.3208/sandf.36.4_1.

Haykin, S. 1999. *Neural Networks, A Comprehensive Foundation*. New York, USA: Macmillan College.

Kurup, P. U., and E. P. Griffin. 2006. "Prediction of Soil Composition from CPT Data Using General Regression Neural Network." *Journal of Computing in Civil Engineering* 20: 281–289. doi:10.1061/(ASCE)0887-3801(2006)20:4(281).

Lee, I. M., and J. H. Lee. 1996. "Prediction of Pile Bearing Capacity Using Artificial Neural Networks." *Computers and Geotechnics* 18 (3): 189–200. doi:10.1016/0266-352X(95)00027-8.

Liao, S. S. C., and R. V. Whitman. 1985. "Overburden Correction Factors for SPT in Sand." *Journal of Geotechnical Engineering, ASCE* 112 (3): 373–377. doi:10.1061/(ASCE)0733-9410(1986)112:3(373).

Liu, Y., J. A. Starzyk, and Z. Zhu. 2008. "Optimized Approximation Algorithm in Neural Networks without Overfitting." *IEEE Transactions Neural Networks* 19 (6): 983–995. doi:10.1109/TNN.2007.915114.

Maizir, H., and K. Kassim. 2013. "Neural Network Application in Prediction of Axial Bearing Capacity of Driven Piles." In Proceedings of the International MultiConference of Engineers and Computer Scientists, Hong Kong.

MathWorks, MATLAB & SIMULINK 2016. generalized regression networks, Accessed December 5 2017 https://www.mathworks.com/help/nnet/ug/generalized-regression-neural-networks.html.

Meyerhof, G. G. 1965. "Shallow Foundations." *Journal of the Soil Mechanics and Foundations Division - ASCE* 91 (2): 21–31.

Mohanty, R., S. Suman, and S. K. Das. 2018. "Prediction of Vertical Pile Capacity of Driven Pile in Cohesionless Soil Using Artificial Intelligence Techniques." *International Journal of Geotechnical Engineering* 12 (2): 209–216. doi:10.1080/19386362.2016.1269043.

Muduli, P. K., S. K. Das, and M. R. Das. 2013. "Prediction of Lateral Load Capacity of Piles Using Extreme Learning Machine." *International Journal of Geotechnical Engineering* 7 (4): 388–394. doi:10.1179/1938636213Z.00000000041.

Neural Planner Software. 2016. *EasyNN Plus*. USA. www.easyNN.com.

Prechelt, L. 2012. "Early Stopping - but When?." In *Neural Networks: Tricks of the Trade*, Edited by Montavon, G., Orr, G., Müller, K-R 53–67. Springer.

Samui, P. 2011. "Prediction of Pile Bearing Capacity Using Support Vector Machine." *International Journal of Geotechnical Engineering* 5 (1): 95–102. doi:10.3328/IJGE.2011.05.01.95-102.

Sarkar, G., S. Siddiqua, R. Banik, and M. Rokonuzzaman. 2015. "Prediction of Soil Type and Standard Penetration Test (SPT) Value in Khulana City, Bangladesh Using General Regression Neural Networks." *Quarterly Journal of Engineering Geology and Hydrology* 48: 190–203.

Shahin, M. A., M. B. Jaska, and H. R. Maier. 2001 March. "Artificial Neural Network Applications in Geotechnical Engineering." *Australian Geomechanics* 36(1): 49–62.

Skempton, A. W. 1986. "Standard Penetration Test Procedures and the Effects in Sands and Overburden Pressure, Relative Density, Particle Size, Aging and over Consolidation." *Geotechnique* 36 (3): 425–447. doi:10.1680/geot.1986.36.3.425.

Specht, D. F. 1991. "A General Regression Neural Network." *IEEE Transactions on Neural Networks* 2 (6): 568–576. doi:10.1109/72.97934.

Suman, S., S. K. Das, and R. Mohanty. 2016. "Prediction of Friction Capacity of Driven Piles in Clay Using Artificial Intelligence Techniques." *International Journal of Geotechnical Engineering* 10 (5): 469–475. doi:10.1080/19386362.2016.1169009.

Terzaghi, K. 1943. *Theoretical Soil Mechanics*. New York: Wiley.

Tomlinson, M., and J. Woodward. 2014. *Pile Design and Construction*. 6th ed. FL, USA: CRC press.

Wolf, P. R., and C. D. Ghilani. 2014. *Elementary Surveying: An Introduction to Geomatics*. 14th ed. Pearson, NJ, USA: Prentice-Hall.